

## THERMAL INERTIA CHARACTERISTICS OF THE MARTIAN CRATER CURIE

*V. M. Horner and J. R. Zimbelman*, Dept. of Geology, Arizona State University, Tempe, AZ, 85287 and Lunar and Planetary Institute, 3303 NASA Rd. One, Houston, TX 77058.

Thermal inertia characteristics have been determined for the martian crater Curie from high resolution groundtracks of Viking Thermal Infrared Mapper (IRTM) data. Curie is located at 28.8° lat, 4.8° long. It is ~120 km in diameter and has an extensive, but somewhat degraded, ejecta blanket. Flow features near the southeastern edge of the ejecta indicate that at least part of the Curie ejecta was emplaced in a manner similar to the ejecta of rampart craters. Curie straddles a boundary between the ridged plains (Hr) and the cratered highlands (Npl<sub>1</sub>), as mapped by (1).

Five high resolution IRTM groundtracks which cross Curie provide coverage of the crater wall, rim and ejecta (fig. 1). They were all obtained between  $L_s = 347^\circ$  and  $L_s = 6^\circ$ , within an hour of local midnight. Emission angles are  $<40^\circ$ . Where the groundtracks overlap, the placement of thermal inertia contours agree to within  $\sim 0.2 \times 10^{-3} \text{ cal cm}^{-2} \text{ sec}^{-1/2} \text{ K}^{-1}$ . The highest thermal inertia values for Curie are obtained for the inner crater wall. Thermal inertia decreases to lowest values just beyond the crater rim, then increases by  $\sim 0.5 \times 10^{-3} \text{ cal cm}^{-2} \text{ sec}^{-1/2} \text{ K}^{-1}$  within the rest of the ejecta unit. The main ejecta unit has lower thermal inertias than the surrounding terrain by  $\sim 0.5 \times 10^{-3} \text{ cal cm}^{-2} \text{ sec}^{-1/2} \text{ K}^{-1}$ . Thus, ejecta near the crater rim is  $\sim 1 \times 10^{-3} \text{ cal cm}^{-2} \text{ sec}^{-1/2} \text{ K}^{-1}$  lower than the surrounding terrain.

Average particle sizes for different units can be derived from thermal inertias. Using the Kieffer et al. model (2), the following average particle sizes are obtained: ridged plains west of Curie = 0.16-0.25 mm, main ejecta unit = 0.13-0.16 mm, near-rim ejecta = 0.10 mm, crater rim =  $\sim 0.3$  mm, inner crater wall =  $\sim 0.4$  mm, and the ridged plains east of Curie = 0.13-0.20 mm. Note, however, that the model assumes a uniform distribution of one particle size. If the calculated particle sizes reflect actual ejecta sizes on Mars, then Curie ejecta should have been eroded beyond detectability, since grain sizes of  $\sim 0.16$  mm are the most easily moved by wind on Mars (3). However, larger blocks are almost certainly incorporated into the thermal inertia signatures; as these would tend to increase thermal inertia values, it can be implied from our observations that the Curie ejecta generally consists of smaller particles and blocks than those within the surrounding terrain.

These observations are consistent with those of Schultz and Mendell (4) for the thermal inertia signatures of lunar crater ejecta. They found that ejecta within a crater radius of the rim of large lunar craters have lower thermal inertia values than the surrounding region. They proposed that the comminution of ejecta particles during emplacement, and their fragmentation upon impact, result in a greater proportion of fine ejecta for large lunar craters than might be expected from scaling the observed ejecta sizes of small explosion craters. This high proportion of smaller particles within the ejecta deposit would result in thermal inertia values lower than those of the surrounding terrain.

Our observations of Curie ejecta might be explained by a similar model. The comminution of ejecta during emplacement and the fragmentation of ejecta upon impact could also result in a large amount of fines for large martian craters. Increased brecciation of ejecta during impact from the vaporization of volatiles within the target material (5,6) may be an additional factor that contributes to the decrease in the average size of ejecta for martian craters.

Block abundances of the region can be obtained from brightness temperatures at different IRTM wavelengths, using a method first developed by Christensen (7). Emissivity-corrected

spectral differences are used to obtain the abundance of hypothetical blocks with a thermal inertia of  $30 \times 10^{-3} \text{ cal cm}^{-2} \text{ sec}^{-1/2} \text{ K}^{-1}$  and an albedo of 0.10. We found that the inner walls and floor of Curie have slightly lower block abundances, on the average, than its surroundings even though their thermal inertias are the highest in the region. These results are similar to recent observations of the dark streak of the crater Pettit, which also has high thermal inertias ( $6-7 \times 10^{-3} \text{ cal cm}^{-2} \text{ sec}^{-1/2} \text{ K}^{-1}$ ) but no difference in block abundance from its surroundings (8). Although no dark material can be seen on the crater walls, the floor of Curie has a region near the central peak which is covered with dark material (fig 1A, unit Ad), and other regions of the floor appear to be darkened by similar materials. Dark 'splotches' within craters have been interpreted as coarse, possible sand-sized material with an anomalously high thermal inertia resulting from its low emissivity (9). Some of the dark material on the floor of the crater may also have been deposited on the crater walls in amounts sufficient to change the brightness temperature, but insufficient for visual detection.

Within the study region there appears to be a general southeastern trend towards lower thermal inertia values (figure 1 b). This trend may be related to the proximity of the Arabia region, which is mainly to the south and east of Curie. Arabia has an extremely low thermal inertia, and is considered to be an area of dust accumulation (7,9). Curie is in a region where the overall thermal inertias change over relatively short distances radial to Arabia (7). Therefore, the observed general decrease in thermal inertia may represent increasing regional dust accumulation in the direction of Arabia. It should be noted that any accumulation of aeolian fines would reduce both the values of thermal inertia throughout the region, as well as the magnitudes of the differences in thermal inertia between the crater rim, the ejecta, and the area surrounding Curie. As only a few centimeters of dust are required to completely obscure the thermal inertia signatures of underlying materials (10), the thermal inertia characteristics of the Curie region may help to provide constraints on the distribution and rates of dust deposition near Arabia.

#### REFERENCES:

- 1) Scott, D. and K. Tanaka, 1986, *1:15M Geologic Map of the Western Region of Mars*, USGS, in press.
- 2) Kieffer, H. H. *et al.*, 1973, *J. Geophys. Res.* **78**, 4291-4312.
- 3) Greeley, R., *et al.*, 1976, *Geophys. Res. Lett.* **3**, 417-420.
- 4) Schultz, P. H. and W. Mendell, 1978, *Proc. Lunar Planet. Sci. Conf. 9th*, 2857-2883.
- 5) Schultz, P. H. and D. E. Gault, 1979, *J. Geophys. Res.* **84**, 7669-7687.
- 6) Wohletz, K. and M. Sheridan, 1983, *Icarus* **56**, 15-37.
- 7) Christensen, P. R., 1982, *J. Geophys. Res.* **87**, 9985-9998.
- 8) Zimbelman, J. R., 1986, *Icarus* **66**, 83-93.
- 9) Zimbelman, J. R. and H. H. Kieffer, 1979, *J. Geophys. Res.* **84**, 8239-8251.
- 10) Jakosky, B. M., 1979, *J. Geophys. Res.* **84**, 8252-8262.
- 11) Witbeck, N. E. and J. R. Underwood, Jr., 1984, *Map I-1614*, USGS.

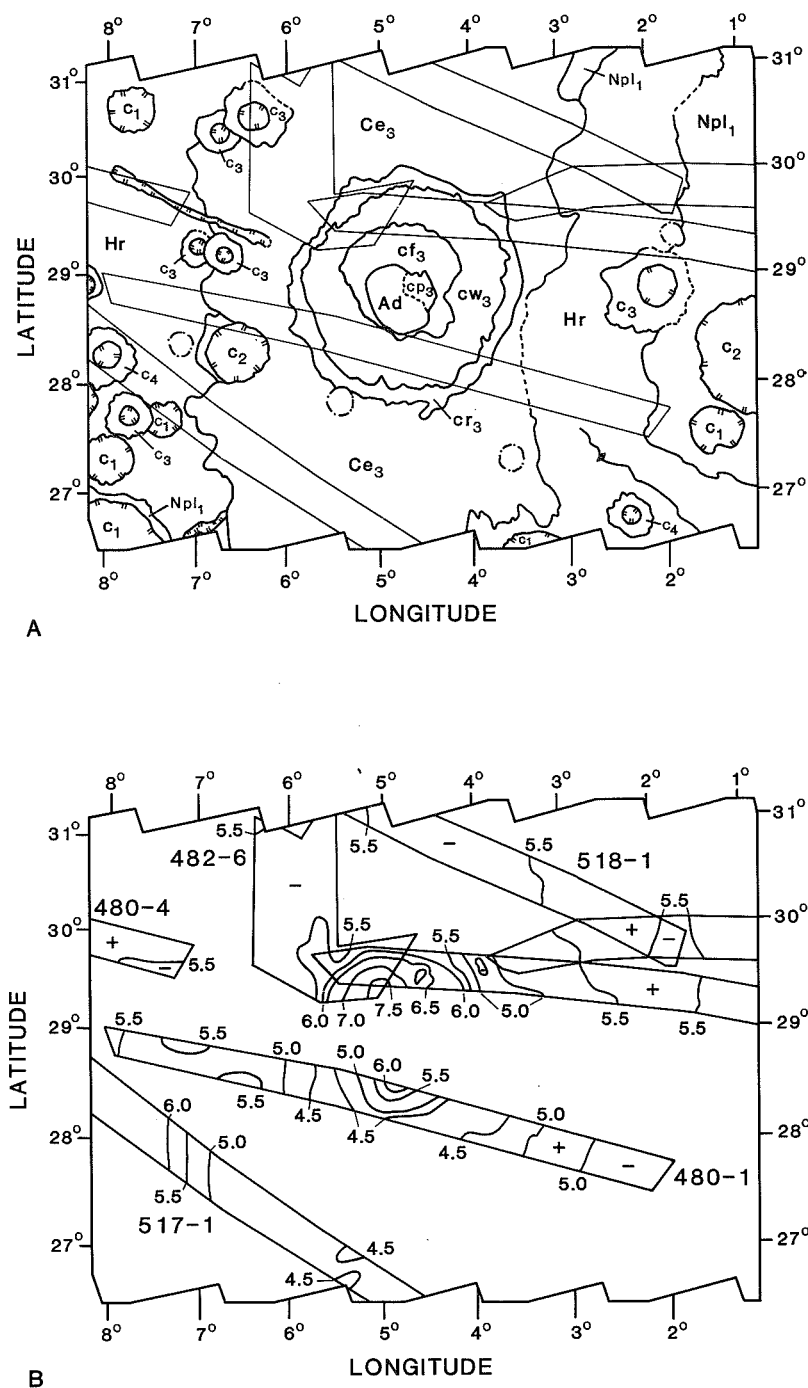


Figure 1 - High resolution Viking IRTM coverage of the crater Curie. Typical resolution  $\sim 25 \text{ km}^2$ , and represents a combination of surface area viewed by each detector and the camera motion along the groundtrack during the integration time. A) Relationship between groundtracks and regional geology; B) Contours of thermal inertia within groundtracks. Geologic units adapted from (1,11). Thermal inertia values are  $\times 10^{-3} \text{ cal cm}^{-2} \text{ sec}^{-1/2} \text{ K}^{-1}$ .